REVIEW ARTICLE

SQUIDs and their applications

J C Gallop and B W Petley
Division of Quantum Metrology, National Physical
Laboratory, Teddington, Middlesex TW11 0LW, UK

Abstract SQUIDs are a class of very sensitive
superconducting measuring devices, whose operation is
based on flux quantization and the Josephson effects. After
a brief summary of these effects the principles of operation
of single and double Josephson junction squids are dealt
with in some detail, including noise processes and estimates
of the ultimate sensitivity attainable. The last part of the
review deals with applications of these devices in a wide
variety of fields including precise electrical measurement,
thermometry, magnetic properties, relativity physics,
geophysical measurement and biomagnetism.

1 Introduction

SQUIDs (Superconducting QUantum Interference Devices)
are a class of very sensitive magnetic flux sensors which may
be used in a variety of applications, ranging from the measure-
ment of very small voltages to the detection of brain waves.
There have already been several excellent reviews of the sub-
ject, of varying complexity (see for example Zimmerman
1972, Clarke 1973, Giffard et al 1972). As well as outlining
the physical principles of flux quantization and the Josephson
effects, on which squids are based, this review describes the
operation of single and double junction devices. We then
attempt to give an up to date analysis of the capabilities and
ultimate limitations of squids, followed by a summary of the
many applications recently proposed for them.

1.1 Flux quantization

The quantization of the magnetic flux linking a super-
conductor was first proposed by London (1950). The electrons
in a superconductor which are responsible for superconduc-
tivity are all in the same macroscopic wavefunction which can
be identified with the complex order parameter Ψ. In the
presence of a magnetic field Ψ behaves just like a single
particle wavefunction so that it is multiplied by a phase factor

$$\exp i(e^*/\hbar) \int A.ds = \exp i\theta$$

where A is the magnetic vector potential at each point in the
superconductor and e^* is the effective charge on the super-
conducting electron charge carriers. The order parameter Ψ,
like any wavefunction, must be single valued so that around
any closed path

$$\oint d\theta = (e^*/\hbar) \oint A.ds,$$
$$= 2n\pi.$$

But by Stokes's theorem

$$\oint A.ds = \int_s B.dS$$
$$= \Phi$$
$$= nh/e^*.$$

Φ is the magnetic flux enclosed by the integration path. For a
simply connected bulk superconductor in an applied field less
than the lowest critical field H_{c1},

$$\Phi = 0$$

but if we take as our model a ring of superconductor in an
external field the flux linking the ring will be

$$\Phi = nh/e^*.$$

That is, it will be quantized in units of h/e^*. For any value of
the external field ($< H_{c1}$) quantization is achieved by a circu-
lating supercurrent flowing on the inner surface of the ring.
This applies a compensating flux which maintains quantization
of the total external and internally generated flux. The small
size of the quantum

$$h/e^* = 2 \times 10^{-15}\ Wb$$

made its detection difficult and it was not achieved until 1961
(Deaver and Fairbank 1961, Doll and Nabauer 1961). The
effective charge e^* was found to be equal to $2e$, a result in
agreement with the microscopic pairing theory of Bardeen,
Cooper and Schrieffer (BCS) (1957).

1.2 The Josephson effects

A year after the observation of flux quantization Josephson
(1962) predicted a number of new and surprising effects in
weakly coupled superconductors. To derive these he con-
sidered the tunnelling of electron pairs through a potential
barrier represented by a thin insulating gap between two bulk
superconductors. If the two are completely separate the phases
of their order parameters θ_1 and θ_2 are decoupled. When the
superconductors are close enough for a weak supercurrent of
electron pairs to pass from one to the other, there is a small
coupling energy which tends to lock the phases together.
A small direct supercurrent i can pass between them and the
phase difference

$$\theta = \theta_1 - \theta_2$$

depends on this current according to

$$i = i_1 \sin \theta. \tag{1}$$

Thus the maximum value of i is i_1 which increases as the
strength of the coupling increases. If a current greater than i_1 is
driven through this 'Josephson junction' from an external

source then a direct voltage V appears across it corresponding to a difference in the chemical potential of the two superconductors. The time dependence of the order parameters, which is just like the Schrödinger equation for two coupled simple harmonic oscillators, shows that in this situation the phase difference is time dependent according to the relationship

$$\dot{\theta} = 2eV/\hbar. \tag{2}$$

Equations (1) and (2) are the relationships derived by Josephson. Substituting (2) into (1) shows that when a junction has a direct voltage V across it an alternating current flows with amplitude i_1 and frequency

$$f = 2eV/h.$$

Josephson's original work dealt with superconductors weakly coupled by pair tunnelling through an insulator. It has been found experimentally that the same properties are shown by a variety of different weak coupling mechanisms, for example superconductors separated by semiconductor or normal metal barriers, thin bridges of superconductor, or junctions made by pressing a pointed superconducting wire onto a flat sheet of superconductor. Some of the more usual junction types are shown in figure 1. Less usual junction types are the solder drop (Clarke 1966), the NbSe₂ platelet weak link (Considori *et al* 1971) and the anodized thin film (Goodkind and Dundon 1971).

2 The single junction SQUID

The simplest SQUID to describe and understand, although historically not the first developed, consists of a superconducting ring of inductance L containing a single Josephson junction with a critical current i_1 (Silver and Zimmerman 1967). To understand the action of the SQUID as a magnetometer we must consider the internal flux state of the ring as a function of an externally applied flux Φ_e. For a uniform strongly coupled ring, starting from zero applied flux the circulating supercurrent i_c increases in step with the external flux so that the total flux linking the ring maintains its original value

$$\Phi_e + Li_c = nh/2e$$
$$= n\Phi_0.$$

For a ring containing a weak link the magnetic flux linking it is no longer exactly quantized. As well as the flux contribution to the phase change of the order parameter around the ring, the circulating screening current will induce an additional phase change across the junction, which may be calculated from equation (1). So the single valued order parameter condition now becomes

$$\Phi_e + Li_c + (2\Phi_0/2\pi) \sin^{-1}(i_c/i_1) = n\Phi_0. \tag{3}$$

This can be solved for

$$\Phi_i = \Phi_e + Li_c$$

as a function of Φ_e in two regimes of interest,

$$2\pi Li_1/\Phi_0 \ll 1$$

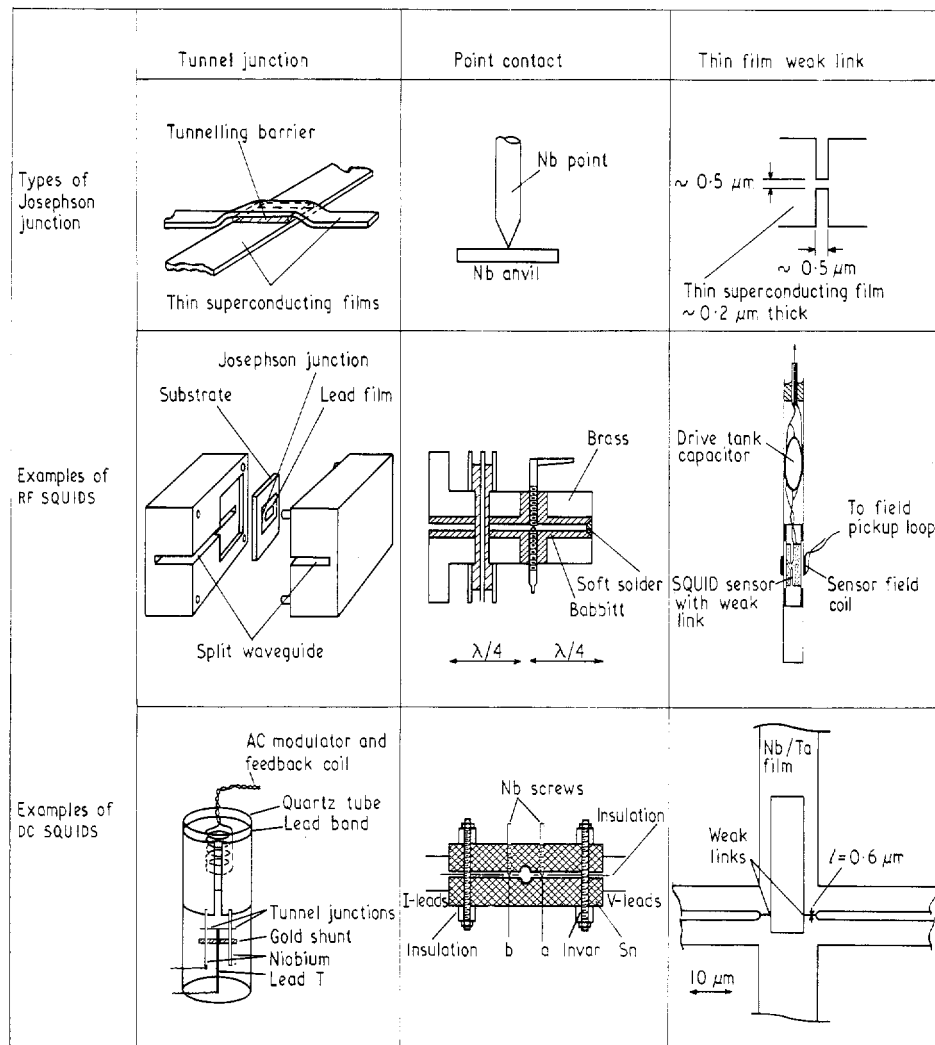|	Tunnel junction	Point contact	Thin film weak link
Types of Josephson junction	Tunnelling barrier Thin superconducting films	Nb point Nb anvil	~ 0·5 μm ~ 0·5 μm Thin superconducting film ~ 0·2 μm thick
Examples of RF SQUIDS	Josephson junction Substrate Lead film Split waveguide	Brass Soft solder Babbitt λ/4 λ/4	Drive tank capacitor To field pickup loop SQUID sensor with weak link Sensor field coil
Examples of DC SQUIDS	AC modulator and feedback coil Quartz tube Lead band Tunnel junctions Gold shunt Niobium Lead T	Nb screws Insulation I-leads V-leads Insulation b a Invar Sn	Nb/Ta film Weak links l = 0·6 μm 10 μm

Figure 1 Types of Josephson junction, with examples of RF and DC SQUIDs incorporating them

and

$$2\pi L i_1/\Phi_0 \geqslant 1.$$

The form of the solutions is shown in figure 2, where we have taken $n = 0$. For the first case the flux quantization is almost
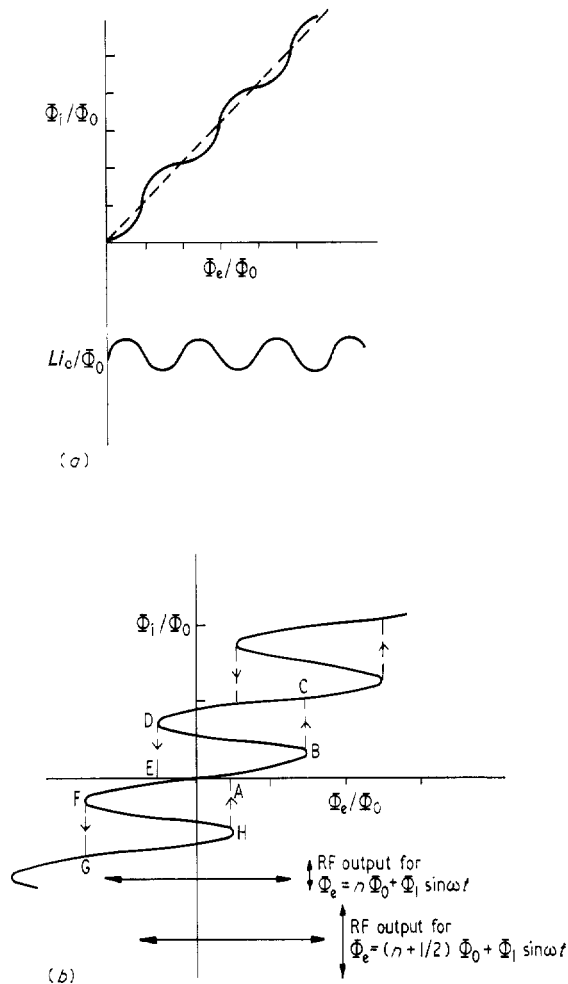

(a)

(b)

Figure 2 (a) The screening effect of a SQUID. Internal flux Φ_i against external applied flux Φ_e for $2\pi L i_1 \ll \Phi_0$. (b) Φ_i against Φ_e for an RF SQUID showing the hysteresis loops and the variation with DC flux of the flux path executed during one RF cycle. In this case $2\pi L i_1 \geqslant \Phi_0$

non-existent. Φ_i follows Φ_e closely, with a small superimposed modulation of periodicity Φ_0. For the second case an attempt at quantization is apparent. As Φ_e increases, the circulating current also increases until it exceeds i_1 whereupon it resets itself to a value less than this. The diagram also shows that in this case Φ_i is a multivalued function of Φ_e in contrast to the situation when $2\pi L i_1/\Phi_0 \ll 1$. Since the internal flux state and circulating current in a SQUID are functions of the applied flux, then to use such a device as a magnetometer or galvanometer we require a sensitive way of interrogating the internal state of the ring. Two distinct interrogation modes have been used for the two regimes dealt with above and these are described in the following two sections.

2.1 The inductive mode

For $2\pi L i_1/\Phi_0 \ll 1$, figure 2 shows that the curve of Φ_i against Φ_e is single valued and in this case the SQUID looks like a parametric inductor with a value L_J which is periodic in the external applied flux and is given by

$$L_J = [\Phi_0 L \sin^{-1}(\Phi_e/L i_1)]/(\Phi_i - \Phi_e).$$

If the SQUID is coupled to a resonant circuit (with inductance L_1, capacitance C and quality factor Q) the resonant frequency ω will depend on the external flux, and will be periodic in it with periodicity Φ_0. The change in resonant frequency can be detected, or for fixed frequency the change in the RF voltage appearing across the tank circuit can be measured. The amplitude of the variation in voltage is given approximately by

$$\Delta V = \omega i_1 (QLL_1)^{1/2}.$$

This is rather small, giving a poor signal to noise ratio with a room temperature amplifier, so that in practical applications this detection mode has been little used.

2.2 The dissipative mode

At present this is the most commonly used mode and forms the basis of operation of all the available SQUID systems. The SQUID ring is again coupled to a resonant circuit with a mutual inductance M and the circuit is driven at a frequency near resonance (see figure 5). Suppose that the DC flux linking the ring is near an integral number of flux quanta. If the RF drive current i_{RF} is increased from zero, then initially the detected RF voltage V_{RF} across the tank coil L_1 also increases linearly. When the drive current amplitude is just greater than $L i_1/MQ$ the SQUID will execute the flux path ABCDEFGHA shown in figure 2 during one cycle of the radiofrequency. This double hysteresis loop causes the dissipation of energy of order $\Phi_0^2/2L$. This is absorbed from the resonant circuit, thereby reducing its level of oscillation.

During the next RF cycle the level will be too low to take the SQUID around the loops but it will build up again over a number of cycles ($\simeq Q$ cycles) until the circulating current is again equal to the critical current of the junction and further energy can be absorbed. A further increase in the RF current amplitude will not now lead to an increase in RF voltage since the only effect is to supply energy faster to the resonant circuit, energy which is more rapidly dissipated by more frequent execution of the hysteresis loops by the SQUID. In fact a further increase in the
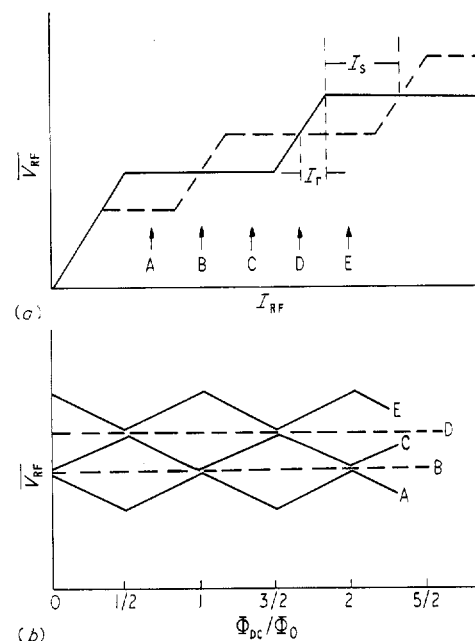

(a)

(b)

Figure 3 (a) Detected RF voltage as a function of RF drive current, the 'staircase' pattern. (b) Variation of the detected RF voltage with applied DC flux for fixed RF drive current, the 'triangle' pattern. —— $\Phi_{DC} = n\Phi_0$, - - - - $\Phi_{DC} = (n+\tfrac{1}{2})\Phi_0$

419

detected voltage does not occur until i_{RF} is large enough to drive the SQUID around A to H once in every RF cycle (point C in figure 3). The length Δi_{RF} of this step is approximately $M\Phi_0/LL_1$. The curve of V_{RF} against i_{RF} has a further linear region following this until a second critical point is reached when another pair of hysteresis loops can be traversed (point E in figure 3). Another flat step follows by the same argument as before so that the whole V_{RF}–i_{RF} curve consists of a series of flat steps separated by an RF voltage of around

$$\Delta V_{RF} = \omega L_1 \Phi_0/M.$$

If now the applied magnetic flux is near $(n+\frac{1}{2})\Phi_0$ and the RF drive current is again increased from zero, then the first transition to a new internal flux state occurs at a value of i_{RF} which is lower by $\Phi_0/2MQ$ than the value when $\Phi_e = n\Phi_0$. Thus the step will occur at an RF voltage which is lower by an amount $\omega L_1 \Phi_0/2M$. This corresponds to the execution of only a single hysteresis loop instead of a double one, due to the asymmetry of the flux pattern about the DC flux level when $\Phi_e = (n+\frac{1}{2})\Phi_0$. Thus this step has only half the width of the others. Further steps correspond to the execution of 3, 5, 7, ... hysteresis loops and so have the normal width. The value of V_{RF} at the step for intermediate flux values is approximately linear in Φ_e between

$$\Phi_e = n\Phi_0$$

and

$$\Phi_e = (n+\frac{1}{2})\Phi_0$$

so that for a fixed RF bias level V_{RF} is a triangular function of external flux as shown in figure 3. As the drive level is increased the triangular pattern grows in amplitude to a maximum, reduces to zero, is phase reversed and increases to a maximum again. This is shown schematically in figure 3 for levels A to E.

The maximum amplitude of the triangular pattern is $\omega L_1 \Phi_0/2M$ as was shown above, and this implies that by reducing M the signal level can be increased. However there is an upper limit set by the condition that the full amplitude of the pattern can only be used if (see figure 3):

$$I_s > I_r.$$

Since

$$I_r = \Phi_0/2MQ$$

and

$$I_s = M\Phi_0/2LL_1$$

this condition reduces to

$$M^2Q/LL_1 \geqslant 1.$$

This shows that the transfer function relating the change in detected RF voltage to a change in the applied flux has a maximum value of

$$\partial V_{RF}/\partial \Phi_e \simeq \omega (QL_1/L)^{1/2}. \tag{4}$$

3 Superconducting rings containing two Josephson junctions

Although this type of device was the first with which superconducting interference effects were observed, it is much less widely used than the single junction devices and, possibly because of this, the theoretical understanding of its mode of operation is less well developed. Here we shall give a brief summary of the theory of operation and discuss in rather more detail the noise processes occurring in two-junction devices.

Consider a superconducting ring of inductance L containing two junctions with critical currents i_1 and i_2 ($i_1 < i_2$). The maximum supercurrent which can be driven through the ring is a periodic function of the magnetic flux applied to the ring, just as for the single junction SQUID. In fact we may plot Φ_i against Φ_e exactly as in figure 2. When no external current is

driven through the two-junction device the flux inside the ring is almost quantized provided that $2\pi Li_1 \gg \Phi_0$, whereas in the opposite limit $\Phi_i \simeq \Phi_e$. In either case the maximum circulating supercurrent which the ring can support is $\simeq i_1$. We can write the phase continuity condition (equation (3)) as

$$2n\pi = \theta_1 - \theta_2 + 2\pi(\Phi_e + Li_c)/\Phi_0.$$

But also

$$Li_c = i_1 \sin \theta_1 - i_2 \sin \theta_2$$

and for $i_1 = i_2$ these equations reduce to

$$Li_c = 2i_1 \{\sin \theta_1 - \sin [\theta_1 + 2\pi(\Phi_e + Li_c)/\Phi_0]\}. \tag{5}$$

In general these equations have no analytic solutions but may be solved numerically or graphically for i_c and Φ_i as functions of Φ_e. For $2\pi Li_1 \gg \Phi_0$, i_c is a multivalued function of Φ_e.

3.1 The finite voltage regime

When a direct current from an external source is driven through the SQUID the situation changes considerably from that of the single SQUID. The external current imposes an extra phase constraint on θ_1 and θ_2 at the two junctions. If the external current is so large that it exceeds the critical current of the double junction then the phases θ_1 and θ_2 become time dependent and a direct voltage appears across the junctions. For a fixed external bias current this direct voltage is a periodic function of the applied external flux and this property forms the basic mode of operation of a double SQUID.

At first the voltage modulation was not understood but it is now seen to result from a straightforward extension of the current biased resistively shunted Josephson junction model (e.g. Giffard *et al* 1972) to the case of two junctions in parallel. In the single junction case the total, constant, current carried by the junction can be divided into a normal and a super-current component

$$i_t = i_s + i_n$$
$$= i_1 \sin \theta + V(t)/R \tag{6}$$

where R is the resistance of the junction in the normal state and $V(t)$ is the instantaneous voltage across the junction and is related to the time dependence of the phase by the second Josephson relationship (equation (2)). For i_t slightly greater than i_1 this results in a periodic, but highly non-sinusoidal variation of θ and $V(t)$ with time, although $V(t) > 0$ for all t.

With two junctions in the superconducting loop an external flux modulates the effective supercurrent component of i_t and since i_t is still fixed V will also be modulated by Φ_e in antiphase with i_s. Figure 4(a) shows a schematic I–V characteristic for a double SQUID in the two cases $\Phi_e = n\Phi_0$ and $\Phi_e = (n+\frac{1}{2})\Phi_0$. The mean voltage as a function of the applied flux Φ_e is also shown. It is an experimental fact that the voltage is periodic in Φ_e and is a single valued function of it and to see why this is so we must rewrite equations (5) and (6) to include a finite voltage across the junctions and see how the circulating supercurrent in the ring varies with time. The total current is now

$$i_t(t) = i_1 (\sin \theta_1 + \sin \theta_2) + V(t)/R$$
$$= 2i_1 \sin [(\theta_1 + \theta_2)/2] \cos [\pi(\Phi_e + Li_c)/\Phi_0] + V(t)/R$$

and the circulating current equation becomes

$$i_c/i_1 = - \sin [\pi(\Phi_e + Li_c)/\Phi_0] \cos [(\theta_1 - \theta_2)_{t=0} - Vt/\Phi_0].$$

The second of these can be solved graphically rather simply and it can be seen that the second term on the right hand side is multiplied by an amplitude factor which is swept from -1 to $+1$ in a highly nonlinear fashion. We can find from a graphical solution the maximum amplitude of the variation of the circulating supercurrent with external flux. The result shows
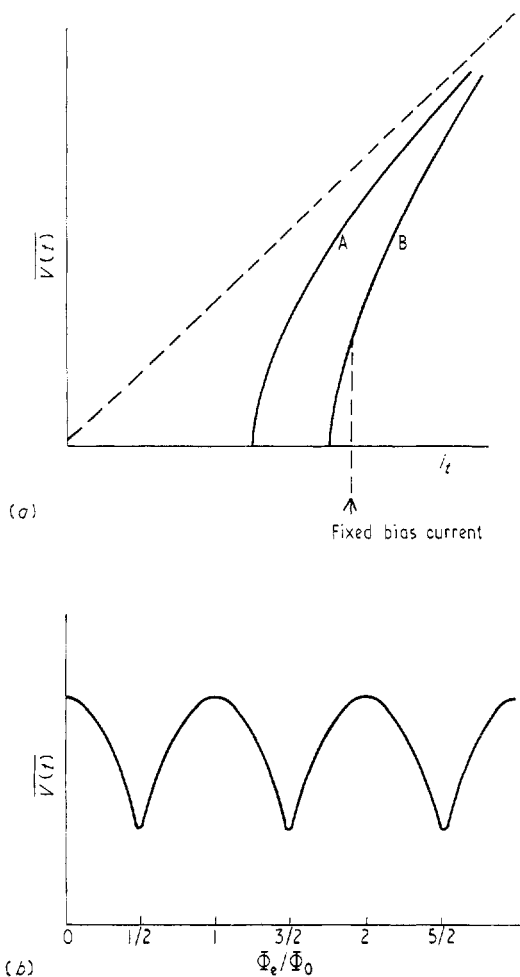
Figure 4 (*a*) Voltage–current characteristic for a DC SQUID, showing its variation with applied DC flux. Curve A: $\Phi_e = (n + \frac{1}{2})\Phi_0$; curve B: $\Phi_e = n\Phi_0$. (*b*) Variation of DC voltage with applied DC flux for fixed bias current

that even when $2\pi L i_1 \gg \Phi_0$, i_c varies only between the limits $-\Phi_0/2L$ and $\Phi_0/2L$. The physical explanation for this result is believed by the authors to be that the metastable state with $i_c > \Phi_0/2L$ cannot be supported by the ring for any significant length of time on the scale of L/R in the finite voltage state since the local energy minimum corresponding to the near quantization of the ring flux near an integral number of Φ_0 goes to zero once during each phase change of 2π. This situation is in contrast to that with θ constant in time for which the metastable states with $i_c > \Phi_0/2L$ will have a very long lifetime.

The limitation on the circulating supercurrent has two consequences. The first is that the maximum change in the device critical current which can be produced by an external flux is limited to Φ_0/L so that the voltage modulation depth ΔV, that is the amplitude of the pattern shown in figure 4, is limited to $\sim R\Phi_0/L$. A second result is that the flux switching contribution to the intrinsic noise in RF SQUIDs is not expected to be present in DC SQUIDs. This is dealt with in more detail in §5.1.2.

4 Comparison of RF and DC SQUIDs

SQUIDs have been constructed using most of the types of Josephson weak-link configuration: tunnel junctions with insulating, semiconducting or metallic barriers, point-contact junctions and metallic thin film bridges as well as crossed wire

and solder drop junctions. The superconducting ring containing the Josephson junctions may be machined from solid metal or may be in the form of a thin evaporated film or a wire.

Many possible arrangements have been used successfully. For the RF SQUID two forms of construction have been widely used and are now available commercially. The first of these, the two-hole SQUID, is an adjustable point-contact device, machined from solid niobium. It is well screened by an external superconducting can and the coil of the resonant circuit is inserted in one hole while a DC current can be sensed by a coil in the other hole. Another very successful form of construction consists of a thin film of superconductor evaporated on the outside of a quartz rod. There is a microbridge constriction in the thin film which forms the junction. Coupling coils may be wound on the outside of the quartz rod. An ingenious design due to Zimmerman (1971) has enabled the intrinsic inductance of the SQUID to be reduced, by connecting a number of superconducting loops in parallel across the Josephson junction (as many as 24 have been used). The arrangement has been compared to an octopus patting itself on the back. Such a multi-hole device, shown in figure 6, yields significantly better signal to noise figures, the improvement being by a factor $n^{1/2}$, where n is the number of loops. Its unusual geometry also means that coupling coils are wound on the outside of the SQUID, which is a particular advantage when bulky or multiturn input coils must be used. In this device the main cylindrical body of the SQUID is in two halves, insulated from each other, except for the junction, which is at the geometric centre of the body, and the spot welded straps which connect the top half to the bottom from one side of each slot to the other. Careful consideration of this complex geometry shows that it reduces to a number of loops in parallel, each containing the Josephson junction.

A block diagram of the detection system frequently used with RF SQUIDs is shown in figure 5. A low frequency modulation ($\simeq 1$ kHz) with amplitude $\Phi_0/2$ is fed to the SQUID
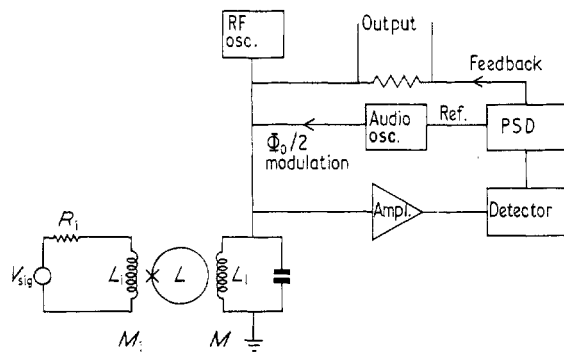

Figure 5 Schematic circuit diagram of RF SQUID galvanometer system, employing feedback

through the resonant circuit and a phase sensitive detector (PSD) gives a DC output which can be fed back to maintain the SQUID locked near an integral number of Φ_0.

The advantages of the point-contact type include operation over a wider range of temperature in general, whereas the thin film device needs no adjustment. Recently work has been reported on preset point-contact junctions which can be temperature cycled many times without readjustment and also thin film bridges have been produced with such small dimensions that the operating temperature range has been considerably extended. So at present it is not clear which design of RF SQUID will prove more popular.

There have been almost as many types of DC SQUID as experiments reported using them. In contrast to the RF device

no preferred designs have emerged. There are probably two reasons for this. It is considerably more difficult (more than twice) to make a double junction SQUID than a single one. In the case of the thin film structure the critical currents must be reasonably matched, while for point contacts it is difficult to make independently adjustable junctions. Added to the construction problems the detection system requires careful design. The double junction with a resistance in the region of 0·1 to 10 Ω must be matched to a low noise amplifier at room temperature. Although noise figures as low as 0·01 dB are attainable, an impedance of around 10 kΩ is required. Transformer matching has been attempted with little success. Recently good matching has been reported (Clarke *et al* 1975a) using a cryogenic resonant circuit. Another approach has been to use the low noise, low input impedance properties of the photocell galvanometer amplifier. Though clearly less convenient in practice, this detection system has allowed even higher magnetic flux resolution to be attained (Gallop 1974). As with the RF SQUID, a feedback detection system is usually used to operate the DC SQUID near fixed flux.

5 Noise in RF and DC SQUIDs

Since SQUID systems show extremely high sensitivity to magnetic fields and electric currents and voltages, one of the most important questions to be answered is how the noise in the system limits this sensitivity. It is generally valid to divide the total noise into that originating in the superconducting ring itself and that in the detector and amplifier system.

5.1 Intrinsic noise in RF SQUIDs

The earliest discussions of intrinsic noise considered the effect of Johnson noise in the normal resistance shunting the Josephson junction. The fluctuating voltage appearing across the junction will give rise to a fluctuating output voltage for both RF and DC SQUIDs which will be equivalent to flux noise, in a bandwidth df, at the input coil of the system of

$$\overline{(\mathrm{d}\Phi^2)}^{1/2} = (4kT\,\mathrm{d}fL^2/R)^{1/2} \tag{7}$$

where R is the normal resistance of the junction(s) which is (are) at temperature T. For typical values this simplest manifestation of thermal noise limits the flux resolution of both types of SQUID to around $5 \times 10^{-7}\ \Phi_0\ \mathrm{Hz}^{-1/2}$.

5.1.1 Flux switching noise in RF SQUIDs
The flux resolution predicted by equation (7) has never been approached by any real system. It has however become apparent through a detailed analysis of the RF SQUID (Kurkijarvi 1972) that the simple shunted junction model is not capable of describing all the thermal noise contributions. There is another contribution present for single junction loops operated in the dissipative mode resulting from an uncertainty in the external flux level at which a quantum is switched into or out of the loop during the execution of a hysteresis loop. The energy barrier against flux entering or leaving goes to zero for $i_c = i_1$ (see figure 2). At finite temperatures thermal excitations cause flux transitions to occur before this barrier reduces to zero. Calculations show that this process gives rise to a flux equivalent noise contribution of the form

$$\overline{(\mathrm{d}\Phi^2)}^{1/2} \simeq 2\,(\mathrm{d}f/\omega)^{1/2}Li_1^{1/3}(2\pi kT/\Phi_0)^{2/3}. \tag{8}$$

For the usual 20 MHz SQUID at 4·2 K this sets a limit on the flux resolution of $1 \times 10^{-4}\ \Phi_0\ \mathrm{Hz}^{-1/2}$, roughly equal to the best which has been achieved in practice. It is clear from equation (8) that increasing the drive frequency causes the limiting flux resolution to decrease rather rapidly. A practical upper limit to the drive frequency is set by the difficulty of obtaining low noise amplifiers operating at microwave frequencies so that the

detection system noise will eventually dominate. The optimum pump frequency is probably around 10 GHz and such a system has allowed a resolution of $10^{-5}\ \Phi_0\ \mathrm{Hz}^{-1/2}$ (Pierce *et al* 1974) comparable with the best DC systems, but still worse than the intrinsic noise limitation set by equation (8) for this frequency.

5.1.2 Thermal noise in DC SQUIDs
No analysis comparable to Kurkijarvi's (1972) has been given for intrinsic noise in DC SQUIDs. We suggest here that flux switching noise does not limit the device sensitivity as it does for the conventional RF SQUID, driven at a pump frequency of 20–30 MHz. In the authors' view the absence of a multivalued Φ_i against Φ_e relationship for the DC device in the finite voltage region (see §3.1) means that there is no thermally excited switching from one metastable flux state to another. A different way of treating the DC SQUID is to regard it as an RF device in which the pump power is generated as a circulating supercurrent at the Josephson frequency V/Φ_0.

A qualitative argument was put forward in §3.1 to show that the magnitude of this pump current is $\leqslant \Phi_0/L$ so that it is incapable of driving flux quanta in or out of the ring. This is supported by some numerical calculations of de Bruyn Ouboter and de Waele (1970). To settle the point finally a more detailed analysis is required, but if flux switching of the type described above were to exist in DC SQUIDs, it would be an insignificant limitation on the ultimate sensitivity. This is because the typical bias voltage used is in the range 10–100 μV, corresponding to a pump frequency in the microwave region. Substituting in equation (8) gives a limiting flux resolution of around $10^{-6}\ \Phi_0\ \mathrm{Hz}^{-1/2}$ in this case.

5.1.3 1/f noise in SQUIDs
A form of flicker noise with a $1/f$ spectral dependence has been observed in a thin film DC SQUID using Nb tunnel junctions (Clarke *et al* 1975b). The origin of the noise appears to be thermal, arising from temperature fluctuations in the junctions themselves which change their critical currents and put noise on the detected junction voltage. The device used had a limiting resolution of $3 \times 10^{-5}\ \Phi_0\ \mathrm{Hz}^{-1/2}$. This may not be typical of all DC SQUIDs since it is thought that the geometry of the junction as well as their sizes may strongly affect the frequency range and magnitude of this particular noise contribution. Recently Clarke *et al* (1975a) have also looked at the frequency dependence of noise in two commercially available RF SQUID systems and have found that for both, $1/f$ noise begins to dominate at around 0·1 to 0·01 Hz, roughly the same as for their DC device. This is interesting since the results show no significant difference between point-contact or thin film devices.

5.1.4 Total system noise and ultimate sensitivity
From the preceding three sections we may conclude that there is no simple 'best buy' when choosing between a DC or RF device if the highest sensitivity is required. At present both types have exhibited comparable flux resolution. The DC detection system required to achieve this is much simpler and cheaper. On the other hand the resonant signal amplification available with RF, as well as the form of equation (8), show that as the noise temperatures of UHF and microwave amplifiers are reduced the single junction types will come into their own, provided that cost is no object. An interesting development relevant to this is the 9 GHz self-pumped parametric amplifier of Kanter (1975). This has a construction which is similar to a resistive microwave SQUID although its mode of operation is not strictly dependent on a SQUID type of quantum interference effect.

The discussion on noise has introduced a number of mechanisms which limit the ultimate sensitivity of SQUIDs, expressed in terms of the minimum resolvable magnetic flux change. In

most real applications an input coil converts the magnetic field, voltage or current to be measured into a flux change at the SQUID sensor. The design of this input coil configuration is at least as important to achieving the highest precision as is optimizing the intrinsic flux sensitivity.

It seems likely that future developments of SQUID detection systems will allow a significant improvement in the flux sensitivity which can be obtained. This may come from an increase in the operating frequency, the use of cryogenic amplification in the detection system or most probably a combination of these. The improvements will probably reach the stage where the noise contributions from the SQUID itself and the detection system are comparable. The added complication of the significant thermal noise in the input circuit means that, for optimum sensitivity, the whole system must be carefully matched. For the simple generalized measurement circuit of figure 5, which could represent a sensitive galvanometer or a picovoltmeter, the total noise energy per unit bandwidth may be written

$$\bar{E}_{tot} = \bar{E}_{input} + \bar{E}_{SQUID} + \bar{E}_{detector}$$
$$= 2kTL_i/R_i + 2kTL/R + K^2\Phi_0^2/2L \qquad (9)$$

where $K\Phi_0$ is the equivalent flux sensitivity of the detection system. One advantage of working with superconducting devices is that stray circuit inductances can be very much reduced, even at zero frequency, by the use of superconducting shields. For the idealized circuit we may write

$$M_i^2 = c^2 L_i L$$

where M_i is the mutual inductance between the input coil and the SQUID and c is the coupling coefficient, which for an optimum design we will take to be 1. This allows equation (9) to be written

$$\bar{E}_{tot} = 2kT(L/R + M_i^2/R_iL) + K^2\Phi_0^2/2L.$$

Note the different functional dependence of each of the terms on L. To minimize $\bar{E}_{tot}$ the following condition must apply

$$L^2/R = (M_i^2/R_i + K^2\Phi_0^2/4kT) \qquad (10)$$

and the minimum energy sensitivity for a signal to noise ratio of 1 then reduces to

$$\bar{E}_{min} = 4kTL/R.$$

This may be further simplified. The SQUID inductance cannot be reduced below that of its parametric inductance L_J which forms the basis of its operation in all three modes, and this means that

$$\bar{E} \geqslant 4kTL_J/R$$
$$= 4kT\Phi_0/Ri_1.$$

There are good theoretical and experimental grounds for believing that for a Josephson junction $Ri_1 \leqslant \pi\Delta/2$ where 2Δ is the BCS energy gap parameter so that $\bar{E}_{min} \geqslant 8kT\Phi_0/\pi\Delta$. Another way of looking at this restriction is that $2\Delta/\Phi_0$ is of the order of the maximum frequency at which Josephson effects are observable since higher frequency photons have sufficient energy to break up Cooper pairs (Bardeen et al 1957). So the maximum sensitivity relationship reduces to the simple expression that the minimum detectable energy per unit bandwidth is that due to thermal noise in a system with two degrees of freedom (input coil plus SQUID) spread throughout the maximum bandwidth available with a Josephson device. For niobium $2\Delta = 2.8$ mV so that at 1 K ideal SQUID system sensitivity is around 10^{-34} J Hz^{-1}, about a factor of 10^4 better than the highest reported figure to date (Pierce et al 1974).

It is interesting to note that the minimum detectable energy per unit bandwidth has the dimensions of action and the idealized sensitivity for a SQUID suggested above is considerably less than the value of Planck's constant h. There would clearly be some violation of the uncertainty principle if it were possible to achieve this sensitivity. The paradox is resolved if it is remembered that the Nyquist noise formula only applies to a Maxwellian distribution of distinguishable particles. The quantum effects of zero point energy and Fermi–Dirac statistics are believed to modify the simple relationship so that the total fluctuation energy E_{Th} becomes

$$E_{Th} = 4\{hf/2 + hf/[\exp(hf/kT) - 1]\} \qquad (11)$$

so that now the minimum detectable energy per unit bandwidth is

$$\bar{E}_{min} = 2h\{1 + 2[\exp(\alpha T_c/T) - 1]^{-1}\}$$

where

$$T_c = \Delta/\alpha k$$

is the superconducting transition temperature and α is a constant, of order unity. This expression just tells us that at all temperatures below T_c the noise in an ideal SQUID system will be significantly limited by zero point energy fluctuations. The theoretical expression (11) has not been experimentally tested and we may speculate that a very sensitive SQUID system might make this possible in the future.

6 Electrical measurements of high precision and accuracy

Although room temperature measurements are in most cases more convenient, by working at liquid helium temperatures one gains not only from the reduced Johnson noise of the circuit components, but also from the unique properties of superconductivity both for screening and for zero resistance leads and switch contacts. A reliable null detector is of course a first requirement and SQUIDs can be made to perform this function very well. We do not propose to discuss all of the possible applications and the ones which are given serve mostly to illustrate the very diverse applications of SQUIDs. It should be stressed that the zero of these devices can be disturbed by switching effects or by electrostatic discharges – even charging from the operator has had an effect – and consequently considerable shielding precautions may be needed if the full sensitivity corresponding to $\sim 10^{-4}\,\Phi_0$ is required over an extended period.

Attempts have been made to reduce the number of parameters which must be specified in order to describe the performance of a device. Thus Clarke et al (1971) have suggested the input resistance and an equivalent noise temperature. It has been argued (Pierce et al 1974), that for a complete system, such as a galvanometer with associated amplifier, the energy sensitivity is a better parameter to specify than the magnetic flux sensitivity, since for constant coupling this is largely independent of the input inductance. It is therefore very useful for comparison purposes. Thus if the minimum detectable flux is $K\Phi_0$ where $K \sim 10^{-4}$–10^{-5}, the minimum detectable current I is $K\Phi_0/M$ where M is the mutual inductance between the coupling coil and the SQUID. The energy sensitivity is then $K^2L_i\Phi_0^2/2M^2$ J Hz^{-1} where L_i is the input inductance. Thus with $L_i = 0.5\ \mu$H, and $I = 2.6$ pA Pierce et al (1974) achieved an energy sensitivity of 2×10^{-30} J Hz^{-1} with their 10 GHz evaporated film SQUID having $K \sim 10^{-5}$. Their energy sensitivity was limited by the noise in the microwave amplifier system and this could be improved by 4 dB by cooling the preamplifier. The above energy sensitivity with $L_i \sim 0.5\ \mu$H corresponds to an equivalent noise temperature of 0.14 K and 0.14 mK for a 1 Ω and 1 mΩ source impedance respectively. The corresponding voltage sensitivity would be 10^{-18} V Hz$^{-1/2}$ for the latter.

6.1 *Measurement of small voltages*

Although the SQUID is essentially a magnetometer, it may be made into a galvanometer (voltmeter, ammeter, null detector etc) by adding a coil connected to the sensing element. The limiting sensitivity depends on the number of turns of the coil and the tightness of the coupling to the magnetometer, but it may be calculated from the flux sensitivity. Thus taking 10^{-4} Φ_0 Hz$^{-1/2}$ as the flux sensitivity then a voltage $N \times 10^{-19}$ V impressed for one second on a tightly coupled N-turn loop would be detectable.

The impedance of such a voltmeter is exceedingly low. Thus a resistance $N^2 L/T \sim N^2 \times 10^{-9}$ Ω (where L is the SQUID inductance) in series with the N-turn coupling loop would begin to degrade the sensitivity by limiting the loop current. For a resistance of this order at 4 K the Johnson noise is $N \times 10^{-16}$ V Hz$^{-1/2}$ with $L \sim 10^{-9}$ H, and this is a thousand times greater than the minimum detectable voltage of the SQUID. Alternatively the intrinsic noise temperature is 4 μK. It is difficult to make N large enough to match large impedances with a two-hole SQUID although an external superconducting transformer may be used. It is rather easier with the multihole type since the coupling coil may be directly wound around the outside of the SQUID.

The uses of SQUIDs in a variety of potentiometric applications have been explored and reviewed by Giffard *et al* (1972). They used a two-hole SQUID of the Zimmerman type in a variety of circuits. Thus by incorporating it into a flux-locked loop a digital voltmeter with subpicovolt sensitivity could be made with a dynamic range extending to 0·1 μV with an input impedance of 10 Ω and a maximum slewing rate 0·04 μV s^{-1}. While this impedance might at first seem rather low by room temperature standards, the system was used in association with much lower impedance circuits. Thus they investigated the Johnson noise from a 44 $\mu\Omega$ resistor ($\sim 5 \times 10^{-14}$ V Hz$^{-1/2}$). Further a resistance of 1 $\mu\Omega$ was measured to 1 in 10^4 with a power dissipation of only 0·25 pW.

The resistive SQUID too has been used to measure very small voltages, for example Borcherts and Silver (1968) studied the superconducting to normal transition in a CuNb alloy system. They measured voltages as low as 10^{-16} V across 10^{-12} Ω in which the Johnson noise at 4 K is about 10^{-17} V Hz$^{-1/2}$. Clarke (1966) and Rumbo (1970) used DC SQUIDs or SLUGs (Superconducting Low inductance Undulating Galvanometers) to measure small voltages, notably thermoelectric potentials. The sensitivity with 10^{-8} Ω in series with the SLUG was 10^{-15} V; the time constant, limited by the SLUG inductance of 10^{-8} H, was 1 s.

6.2 *The measurement of small currents*

The current sensitivity of SQUIDs is not at first sight quite as impressive as the voltage sensitivity since it is only in the region of a few tenths of a nano-ampere turn in a 1 s time constant. However the impedance is rather low ($\simeq 1$ nΩ) and it is in this aspect that the SQUID is considerably better than competing devices. The current sensitivity may be increased by winding on a large number of turns and this is particularly the case with multihole SQUIDs. Even with the single or double hole types a superconducting transformer may be employed (Clarke *et al* 1971), thereby increasing the current sensitivity although restricting the frequency response.

6.3 *DC current comparator*

The Kusters (1964) DC current comparator lends itself very well to modification for low temperature operation since the design and operation become greatly simplified. The principle of the low temperature method is that two transformer windings are on a single core, arranged such that a DC current in one produces a magnetic flux which balances the flux produced by the

other. A SQUID is used to sense the zero flux condition. The main experimental problem stems from the need to make the windings effectively occupy the same position. This is achieved at low temperatures by enclosing the wires in a superconducting sheath. The first such system was described by Harvey (1972, Harvey and Collins 1973) who achieved 1 : 1 and 10 : 1 ratios which were exact to a few parts in 10^8 for energizing currents of 50 mA. Other systems have since been described by Sullivan and Dziuba (1974) and Grohman *et al* (1973) and precisions of parts in 10^{10} have been claimed using both single and multihole SQUIDs as flux sensors. These devices are useful for establishing exact resistance ratios and for measuring the power coefficients of resistors. The major experimental problem seems to stem from the need to cool the system through the transition temperature very slowly to avoid flux pinning and if this is done the devices allow current ratios to be established to parts in 10^{10}. Sullivan and Dziuba (1974) made a binary transformer which gave ratios of up to 160 : 1 with parts in 10^9 precision. The current sensitivity for a unity ratio winding was 32 pA or alternatively about 0·5 nA turns.

6.4 *The microwave SQUID*

The SQUID should not be thought of as being suitable only for use as a null detector and nowhere is this better exemplified than in the microwave SQUID of Kamper and Simmonds (1972) which was developed at the National Bureau of Standards. The initial intention was to build a SQUID which operated at a higher frequency in order to achieve a better signal to noise ratio, as expected from equation (4). This property was indeed found but in addition the reflected microwave power was found to be a sinusoidal function of the magnetic flux in contrast to the triangular response found at lower frequencies. The original device was made to operate at 9 GHz and is illustrated in figure 1. The point contact was located a quarter wavelength from the end of a shorted section of waveguide which was made from a superconducting material, Babbit (an alloy of lead, tin and antimony). The waveguide was tapered down to about a quarter of a millimetre in order to provide a better impedance match to the point contact. An RF cable passed across the waveguide a further quarter wavelength from the point contact. The incident microwave power was adjusted to be Φ_0 peak to peak (~ 10 pW) and the magnetic field from a current I in the RF wire modulated the reflected microwave power P as

$$P = P_0 + P_1 \sin (2\pi I/I_0).$$

I_0 is the current required to induce a flux quantum in the superconducting loop containing the point contact and the shorted end of the superconducting waveguide. As mentioned earlier the sinusoidal approximation was found to be remarkably good; for example, the second and third harmonics have been observed to be 25 dB and 40 dB respectively down on the fundamental. Consequently if the current I is an alternating current $I(1) \sin \omega t$, the above equation becomes

$$P = P_0 + P_1 \sin [2\pi (I(1)/I_0) \sin \omega t]$$

and the averaged reflected power varies as the zero-order Bessel function $J_0(x)$ (with the first sideband as $J_1(x)$ etc). The zero crossings of these Bessel functions are readily available from tables or may be computed (few tables go as far as the thousandth zero). Hence the ratios of the RF currents at the zero crossings may be computed and the device used to calibrate an attenuator. Thus the current change between the first and second zero of $J_0(2\pi I/I_0)$ corresponds to a change of 6·21722 dB while between the 99th and 100th zero it is approximately 0·1 dB (see figure 7). The ratio of the first to the hundredth zero corresponds to a dynamic range of 45 dB and the first to thousandth zero to about 60 dB. This last figure
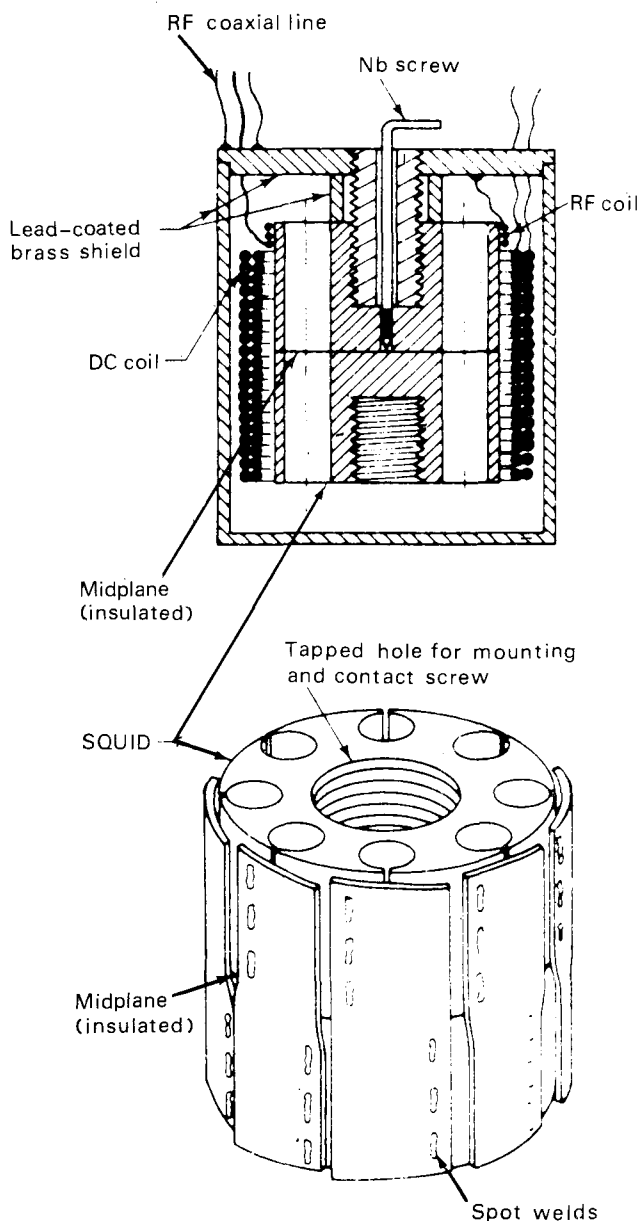
Figure 6 Perspective drawing of an 8-hole SQUID, showing the spot welded niobium straps linking the two cylindrical halves which are insulated from one another across the midplane apart from the point-contact Josephson junction (after Zimmermann)

Figure 7 Microwave SQUID output as a function of RF current amplitude i at 30 MHz (8·9 GHz, − 30 MHz RF, + 1 kHz squarewave $\Phi_0/2$ peak to peak, PSD 0·1 s). The response has a very accurate zero-order Bessel function dependence (J_0). (Note that on this diagram the current scale is nonlinear for small values of i.) ○, J_{01}: 0 dB; ●, J_{02}: + 7·217 dB; ▲, J_{03}: + 11·122 dB; ■, J_{04}: + 13·810 dB; ▼, $J_{0,50}$: + 36·257 dB; *, $J_{0,100}$: + 42·228 dB

band detection techniques to be employed. The sinusoidal response is improved if a normal-metal layer is evaporated onto the post, thereby adding a shunt conductance across the point contact.

6.5 The measurement of $2e/h$

One of the most spectacular applications of the Josephson effects has been their application to the measurement of the atomic constant $2e/h$ and their subsequent use in several national standards laboratories as a quantum method of maintaining the SI unit of potential. The experiment essentially consists of irradiating a Josephson junction with microwaves, and biasing it onto a high order current step. The resulting potential difference across the junction, of between 1 and 10 mV, is then compared with the EMF of a standard cell. This comparison is typically effected by passing the same current through two resistors and simultaneously balancing the standard cell and junction voltages across them.

For the earlier work the resistors, switches and galvanometers were at room temperature. Recently however, systems have been developed in which the essential parts of the potentiometric apparatus are in the cryostat. Sullivan (1972) described a prototype system which worked with a precision of about 1 PPM. The first sub-PPM system was described by Gallop and Petley (1973, 1974) and further systems have been described by Kose *et al* (1974) and Dziuba *et al* (1974). Apart from that of Gallop and Petley, where the galvanometer was an entirely DC biased SLUG, the remainder have used RF SQUIDs as the galvanometer. The overall precisions are believed to be at the part in 10^8 level, although this is difficult to establish reliably and it should perhaps be remembered that at the time of the earlier work (Parker *et al* 1969, Petley and Morris 1970), measurement of a potential of around 1 mV to 1 PPM was considered to be the limit of accuracy.

7 Temperature measurement with SQUIDs

A number of different methods have been used in conjunction with SQUIDs for the measurement of temperature, for there are many properties which change with temperature. For example the temperature variation of the magnetic susceptibility of a paramagnetic material which obeys Curie's law ($\chi \propto 1/T$) provides a way of extending temperature scales below the liquid helium vapour pressure scale. The material must be

represents about the practical limit of the range for attenuator calibration. Using the SQUID in this way, Kamper *et al* (1974) were able to calibrate a 30 MHz coaxial piston attenuator to better than 0·002 dB over a 45 dB range. (Petley *et al* (1976) have achieved a similar precision with their moulded SQUID.) Various ways have been tried to increase the current sensitivity from about one flux quantum per 100 μA by using a toroidal RF coupling coil. This results in a reduction of the bandwidth which, in the broadband version, extends from DC to 1·5 GHz. In principle it should be possible to calibrate attenuators over a wide frequency range. One of the present disadvantages of the method lies in the unpredictable variations in the harmonic content which affect the calibration precision considerably. The harmonic content may be minimized by adjusting the DC current in the RF line and also by optimizing the amplitude of the 10 kHz squarewave modulation. The latter is added to the RF signal to enable narrow-
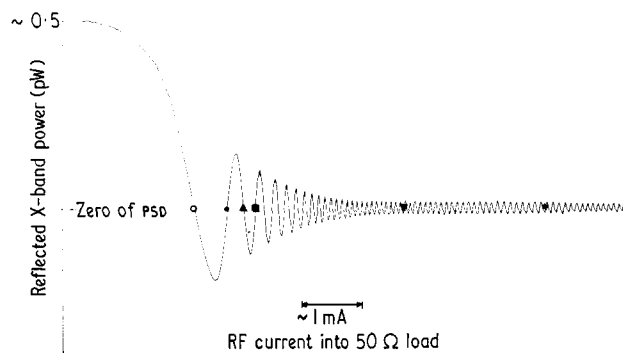
magnetically weak if it is not to order at temperatures above the millikelvin region.

However by using a squid, Giffard *et al* (1972) were able to measure the susceptibility of only a few milligrams of cerium magnesium nitrate in order to make temperature measurements between 5 mK and 4·2 K in flux densities as low as 200 μT. Similarly they measured the paramagnetic nuclear susceptibility of copper, which obeys Curie's law down to microkelvin temperatures and has been used up to 0·1 K, allowing comparison with other temperature scales. The NMR signal from copper has also been explored as a method of temperature measurement (§8.3).

A further possibility is to use the Johnson noise voltage from a resistor R, in a bandwidth df which varies as $(4kTR\,df)^{1/2}$, as a method of temperature measurement. There are two ways of doing this; either to incorporate the resistor in the construction of the squid and to look at the frequency spectrum of the resulting Josephson oscillation (Kamper *et al* 1971), or to couple the voltage variations as flux variations in a conventional squid (Gifford *et al* 1972).

Kamper *et al* (1971) showed that it was possible to measure temperatures between 3 and 23 mK with submillikelvin precision. Their basic method was to take a single turn squid and insert a 10 $\mu\Omega$ brass section in the loop. The device was then biased to give a Josephson oscillation frequency of 30 MHz on which was superimposed the frequency modulation resulting from the Johnson noise. The signal was amplified and fed to a computing counter and the temperature obtained from the bandwidth df by the relationship

$$df = 4\pi kTR/\Phi_0^2.$$

A very careful comparison between such a noise thermometer and another absolute millikelvin device, the nuclear orientation thermometer, has been reported by Soulen and Marshak (1975). This showed agreement to about $\pm 0\cdot5$ mK in the range from 12 mK to 35 mK.

Soulen and Finnegan (1974) have reported preliminary work using a resistive microwave squid for noise thermometry. They inserted a 3 $\mu\Omega$ section around the point contact. The bias voltage of 2 nV gave a 1 MHz oscillation frequency which appeared as 20% AM sidebands on the 10 GHz reflected signal.

8 Magnetization measurements

The extremely high flux sensitivity of squids is obviously useful for measuring very small magnetizations. Magnetic impurity states in transition metal alloys may be directly observed (Fickett and Sullivan 1974) as can the weak magnetism of some biological molecules (Hoenig *et al* 1972). Even the very weak nuclear magnetization of liquid ^{3}He below the superfluid transition has been accurately measured in an external field of 0·05 T (Halperin *et al* 1973).

8.1 Gravimeter

Prothero and Goodkind (1968) described a gravimeter which uses the levitation of a superconducting sphere by the 0·021 T field produced by persistent supercurrents. The constancy of the levitating flux is ensured by a squid magnetometer and a capacitance probe is used to sense changes in the degree of levitation. Goodkind and Warburton (1975) reported a stability of a few parts in 10^{10} per day for $\delta g/g$ measurements. It is hoped to use the gravimeter as a method of earthquake prediction and this requires detecting changes of a few parts in 10^9 per month. This is based on the assumption that strain prior to an earthquake will cause the surface to rise locally with a consequent change in g.

8.2 Gravity wave detector

A squid is being used as a detector of very small mechanical movements in a sophisticated gravity wave detector (Boughn *et al* 1975). A large aluminium bar, coated with superconductor, is cooled to liquid helium temperatures and levitated. A superconducting diaphragm, bonded to one end of the bar, is magnetically coupled to a pair of superconducting coils carrying a current. Relative movement of coil and diaphragm at the resonant frequency of the bar, as would be caused by absorption of a graviton, causes a modulation of the supercurrent, which may be detected by the squid. This system has allowed the antenna noise temperature to be reduced by a factor of ~ 20 over conventional detectors.

8.3 Gyroscope

Hendricks (1975) has described a proposed cryogenic gyroscope system which is to be used for an orbiting-gyroscope relativity experiment. The gyroscope will incorporate a squid as a sensor and a resolution of $10^{-4}\,\Phi_0$ would correspond to an angular resolution of $3\cdot5 \times 10^{-3}{''}$. The principle of the device is that a superconducting sphere is electrostatically levitated and caused to spin with angular frequency ω. The spin generates an internal magnetic field (London moment)

$$\mathbf{B}_\mathrm{L} = (2m/e)\omega = 1\cdot137 \times 10^{-11}\omega \text{ T}.$$

For the 38 mm diameter sphere which is to be used the flux induced in a loop which is essentially perpendicular to the spin axis is 5871 Φ_0. The relativistic precession rates that are being looked for are, for a 500 nautical mile polar orbit, 6·3$''$ per year and 0·05$''$ per year, for the motion of the gyroscope about the earth and rotation of the earth itself, respectively. For a polar orbit the two precession effects are perpendicular and two systems which are perpendicular will discriminate the two effects.

A second possibility which is being developed is the replacement of the spinning levitated sphere by a ^{3}He sample. The nuclear spins have a very long relaxation time in the absence of external perturbations. Provided that the superconducting shielding can exclude magnetic fields sufficiently, the spin axis should persist for several years.

The major obstacle to the general adoption of superconducting gyroscopes stems from the AC loss in superconductors which exists even at quite modest fields thereby preventing the gyroscope from being entirely frictionless.

8.4 Observation of NMR with SQUIDs

Day (1972) reported using a squid magnetometer to detect fast passage NMR signals from lithium and fluorine in LiF and from protons in water at room temperature with an applied flux density of 0·75 T. The RF power required for maximum signal from LiF was 40 dB less than that required for maximum signal using conventional adiabatic fast passage methods. That is, lines 0·8 mT wide were detected at full intensity using 5 μT RF amplitude.

Meredith *et al* (1973) have described the application of a squid to the detection of nuclear magnetic resonance signals below 1 K. Their analysis showed that the squid detection method should be more sensitive than conventional methods at low frequencies and for long relaxation times. Thus for copper at 1 K with $T_1 = 1$ s and $T_2 = 10$ s the squid method becomes more sensitive below 25 MHz ($2T$). The method could be used as a nuclear thermometer either by observing the signal amplitude, which varies as T or the spin–lattice relaxation time which varies as T^{-1}.

8.5 Radiation detection

SQUIDs have been used in conjunction with bolometers as detectors of far infrared radiation. Thus Clarke *et al* (1974)

using a superconducting tunnel junction bolometer obtained a noise equivalent power (NEP) of 5×10^{-15} W Hz^{-1} with a 3 s time constant for frequencies between 1 and 50 cm^{-1}. One must of course use cooled narrow-band filters to exclude broadband blackbody radiation. They suggest that a fivefold improvement in the sensitivity can be achieved together with a 10 Hz bandwidth with a detector area of 0·3 cm^2.

8.6 Geophysical applications

SQUID magnetometers have been shown to be capable of measuring several parameters of interest to earth scientists. Buxton and Fraser-Smith (1974) measured ultra-low frequency fluctuations in the earth's magnetic field. A similar portable SQUID system has been compared with a number of conventional instruments for earth field measurements (Zimmerman and Campbell 1975). The high sensitivity, linearity and dynamic range of the former were found to be particularly useful and the SQUID performance was superior to that of the other systems at all frequencies below about 10 Hz.

Measurements of the time dependence of the earth's field made by SQUID sensors simultaneously at two different sites can yield information about the subsurface resistivity, a parameter which has relevance to geophysical prospecting (Frederick *et al* 1974).

9 Magnetic field gradients

The double and multihole SQUIDs have the virtue of being sensitive to magnetic field gradients (at least for some configurations of the latter), but for many purposes an external pair of oppositely wound search coils must be used. These must be well balanced if they are to be sensitive only to magnetic field gradients. Difficulties were experienced at first with achieving an exact balance which remained stable with time. However Zimmerman and Frederick (1972) found that by making the superconducting transformer with many turns of fine wire they restricted the freedom of movement of the trapped flux. They achieved a stability of balance of parts in 10^5 which gave a sensitivity of 10^{-4} Φ_0 in the presence of the 10^{-11} T fluctuations in the earth's magnetic field.

Representative sensitivities to gradient corresponding to a SQUID sensitivity of 10^{-4} Φ_0 are 10^{-14} T m^{-1} $Hz^{-1/2}$ for 0·1 m diameter loops separated by 0·1 m and a coupling factor to the SQUID of 0·2.

9.1 Magnetocardiography and magnetoencephalography

An impressive application of field gradient detection has been the development of the new subject of magnetocardiography. Cohen *et al* (1970) detected the 10^{-11} T peak amplitude magnetic field signal from the human heartbeat. Subsequent work showed that the SQUID could be operated in a normal environment provided that the vibration level was not too high. Opfer *et al* (1974) have described a Dayem bridge type of second derivative SQUID magnetometer which was suitable for operation in a commercial type environment where the ambient field at 60 Hz was 3×10^{-8} T. They discuss in their paper the effects of coil imbalance as the source distance is varied. They were also able to observe remanent magnetization of $\simeq 10^{-10}$ T following the application of a 10^{-1} T flux density to the subject. This had been reported earlier by Zimmerman and Frederick (1971). Table 1 shows the magnetic field fluctuation levels for various environments compared with the field levels from several physiological sources. Magnetocardiographs (MCGs) provide more detailed information about heartbeats than do electrocardiograms (ECGs). The SQUID technique also has the advantage of being non-contacting. This is a great advantage in examining foetal hearts where the MCG allows much easier discrimination between foetal and

Table 1 This table shows a comparison of the magnetic fields arising from various biological magnetic activities with typical magnetic noise levels in various environments. The bandwidths for measurements and noise are typically DC to 50 Hz. (Information supplied by Dr J Ahopelto.) The comparison demonstrates the need for a gradiometer system to discriminate against noise

Field (nT)	Biomagnetic source	Environment noise level
100		Typical laboratory
10		
1		Quiet site
0·1	Ferromagnetic particles in lung	Earth's field fluctuation
0·01	Adult MCG	
0·001	Foetal MCG	
0·0001	Brain waves, muscle activity	
0·00001		Lowest SQUID noise to date

maternal beats than does the ECG. Figure 8(*a*) shows such a comparison carried out by Ahopelto *et al* (1975) in a magnetically unshielded but quiet environment, using a 450 MHz SQUID. Magnetic fields resulting from electrical activity of the brain have also been observed with SQUIDs (see figure 8(*b*)). This interesting work is still at an early stage.

(*a*)

(*b*) Eyes open: weak α Eyes closed
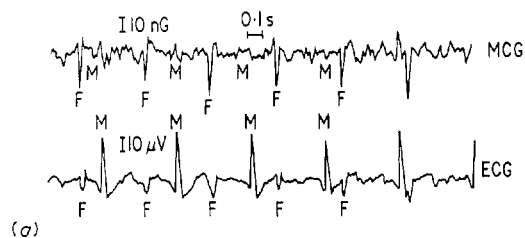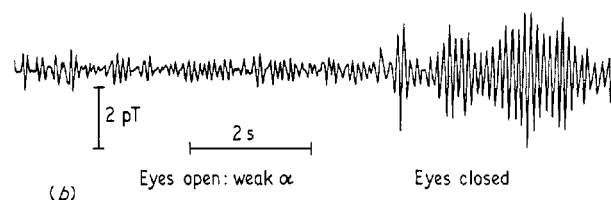
Figure 8 (*a*) Comparison of SQUID foetal MCG and conventional foetal ECG. The SQUID trace shows the foetal heartbeat (F) in more detail than the maternal beat (M) in contrast to the situation with the ECG.
(*b*) Magnetoencephalograph showing variation of brain α rhythms (Ahopelto *et al* 1975)

9.2 Magnetic dipole detection and tracking

If the five independent components of the magnetic field gradient tensor can be determined at a single point it is possible to deduce the strength and spatial distribution of the dipoles giving rise to the gradient (Wynn *et al* 1975). These authors have built a SQUID gradiometer to do this, together with the computing facilities to carry out the transformation. This prototype system, although at present limited to a sensitivity

of 3×10^{-14} T m^{-1} Hz$^{-1/2}$ has been used to plot movements of a truck at a distance of 100 m from the sensor.

10 Future developments

We have in this review attempted to illustrate the very diverse areas in which SQUIDs have already been applied in measurements of both high precision and accuracy. In so doing we have been obliged to be selective and consequently some uses have been omitted. As has been demonstrated here, the future applications will probably be limited by the ingenuity of the experimenter rather than by the SQUID itself. The inherent need to use liquid helium need not in itself be a disadvantage and small portable cryostats have already been described by Zimmerman and Siegwarth (1973). More reliable SQUIDs using preset encapsulated point contacts or evaporated films with either weak links or tunnel junctions have been described. The reliability of SQUIDs has been improved considerably and some types are now available commercially. Several groups are working on high frequency RF SQUIDs to improve their sensitivity further.

It seems very probable that all these new developments will combine to yield many more interesting applications of SQUIDs in the future.

References

Ahopelto J, Karp P J, Katila T E, Lukander R and Makipaa P 1975 *Proc. 14th Int. Conf. Low Temp. Phys.* vol 4 (Amsterdam: North-Holland) pp 262–5

Bardeen J, Cooper L N and Schrieffer J R 1957 *Phys. Rev.* **108** 1175–208

Borcherts R and Silver A H 1968 *Bull. Am. Phys. Soc.* **13** 379

Boughn S P, McAshan M S, Paik H J, Taber R C, Fairbank W M and Giffard R P 1975 *Proc. 14th Int. Conf. Low Temp. Phys.* vol 4 (Amsterdam: North-Holland) pp 246–9

de Bruyn Ouboter R and de Waele A Th 1970 *Prog. Low Temp. Phys.* **5** 243–90

Buxton J L and Fraser-Smith A O 1974 *IEEE Trans. Geosci. Electron.* **GE12** 109–13

Clarke J 1966 *Phil. Mag.* **13** 115–27

Clarke J 1972 *Proc. IEEE* **61** 1–35

Clarke J, Goubau W M and Ketchen M B 1975a *IEEE Trans. Magn.* **MAG11** 724–7

Clarke J, Goubau W M and Ketchen M B 1975b *Proc. 14th Int. Conf. Low Temp. Phys.* vol 4 (Amsterdam: North-Holland) pp 214–7

Clarke J, Hoffer G I and Richards P L 1974 *Rev. Phys. Appl.* **9** 69–71

Clarke J, Tennant W E and Woody D 1971 *J. Appl. Phys.* **42** 3859–65

Cohen D, Edelsack E A and Zimmerman J E 1970 *Appl. Phys. Lett.* **16** 278–80

Considori F, Fife A A, Frindt R F and Gygax S 1971 *Appl. Phys. Lett.* **18** 233–5

Day E P 1972 *Phys. Rev. Lett.* **29** 540–2

Deaver B S Jr and Fairbank W M 1961 *Phys. Rev. Lett.* **7** 43–6

Doll R and Nabauer M 1961 *Phys. Rev. Lett.* **7** 51–4

Dziuba R F, Field B F and Finnegan T F 1974 *IEEE Trans. Instrum. Meas.* **IM23** 264–7

Fickett F R and Sullivan D B 1974 *J. Phys. F: Metal Phys.* **4** 900–5

Frederick N V, Stanley W D and Zimmerman J E 1974 *IEEE Trans. Geosci. Electron.* **GE12** 102–3

Gallop J C 1974 *J. Phys. E: Sci. Instrum.* **7** 855–9

Gallop J C and Petley B W 1973 *Electron. Lett.* **9** 488–9

Gallop J C and Petley B W 1974 *IEEE Trans. Instrum. Meas.* **IM23** 267–71

Giffard R P, Webb R A and Wheatley J C 1972 *J. Low Temp. Phys.* **6** 533–610

Goodkind J M and Dundon J M 1971 *Rev. Sci. Instrum.* **42** 1264–5

Goodkind J M and Warburton R J 1975 *IEEE Trans. Magn.* **MAG11** 708–11

Grohmann K, Hahlbohm H D, Gubbig H and Ramin H 1973 *PTB Mitt.* **83** 313–8

Halperin W P, Buhrmann R A, Richardson R C and Lee D M 1973 *Phys. Lett.* A **45** 233–4

Harvey I K 1972 *Rev. Sci. Instrum.* **43** 1626–9

Harvey I K and Collins H O 1973 *Rev. Sci. Instrum.* **44** 1700–2

Hendricks J B 1975 *IEEE Trans. Magn.* **MAG11** 712–5

Hoenig H E, Wang R H, Rossman G R and Mercereau J E 1972 *Proc. Appl. Superconductivity Conf., Annapolis* pp 570–4

Josephson B D 1962 *Phys. Lett.* **1** 251–3

Kamper R A, Siegwarth J D, Radebaugh R and Zimmerman J E 1971 *Proc. IEEE* **59** 1368–9

Kamper R A and Simmonds M B 1972 *Appl. Phys. Lett.* **20** 270–2

Kamper R A, Simmonds M B, Adair R T and Hoer C A 1974 *NBS Tech. Note 661*

Kanter H 1975 *J. Appl. Phys.* **46** 4018–25

Kose V, Melchert F, Engelland W, Fack H, Fuhrmann B, Gutmann P and Warnecke P 1974 *IEEE Trans. Instrum. Meas.* **IM23** 271–5

Kurkijarvi J 1972 *Phys. Rev.* B **6** 832–5

Kusters N L 1964 *IEEE Trans. Instrum. Meas.* **IM13** 197–209

London F 1950 *Superfluids* vol 1 (New York: Wiley)

Meredith D J, Pickett G R and Symko O G 1973 *J. Low Temp. Phys.* **13** 607–15

Opfer J E, Yeo Y K, Pierce J M and Rorden L H 1974 *IEEE Trans. Magn.* **MAG10** 536–9

Parker W H, Langenberg D N, Denenstein A and Taylor B N 1969 *Phys. Rev.* **177** 639–64

Petley B W and Morris K 1970 *Metrologia* **6** 46–51

Petley B W, Morris K, Yell R W and Clarke R N 1976 *Electron. Lett.* **12** 237–8

Pierce J M, Opfer J E and Rorden L H 1974 *IEEE Trans. Magn.* **MAG10** 599–602

Prothero W A and Goodkind J M 1968 *Rev. Sci. Instrum.* **39** 1257–62

Rumbo J 1970 *Phil. Mag.* **22** 953–64

Silver A H and Zimmerman J E 1967 *Phys. Rev.* **157** 317–41

Soulen R J and Finnegan T F 1974 *Rev. Phys. Appl.* **9** 305–7

Soulen R J and Marshak H 1975 *Proc. 14th Int. Conf. Low Temp. Phys.* vol 4 (Amsterdam: North-Holland) pp 60–3

Sullivan D B 1972 *Rev. Sci. Instrum.* **42** 612–3

Sullivan D B and Dziuba R F 1974 *Rev. Sci. Instrum.* **45** 517–9

Wynn W M, Frahm C P, Carroll P J, Clark R H, Wellhoner J and Wynn M J 1975 *IEEE Trans. Magn.* **MAG11** 701–7

Zimmerman J E 1971 *J. Appl. Phys.* **42** 4483–7

Zimmerman J E 1972 *Cryogenics* **12** 9–31

Zimmerman J E and Campbell W H 1975 *Geophys.* **40** 269–83

Zimmerman J E and Frederick N V 1971 *Appl. Phys. Lett.* **19** 16–9

Zimmerman J E and Frederick N V 1972 *NBS Report* 10736

Zimmerman J E and Siegwarth J D 1973 *Cryogenics* **13** 158–9

Zimmerman J E, Thiene P and Harding J T 1970 *J. Appl. Phys.* **41** 1572–80